Dynamical behavior of three-dimensional confined Ising systems with short- and long-range competing surface fields

M. V. Manias,[1] A. De Virgiliis,[2,3] E. V. Albano,[2,3] M. Müller,[4] and K. Binder[3]
[1]*IFLP, Departamento de Física, UNLP, La Plata, Argentina*
[2]*Instituto de Investigaciones Fisicoquímicas Teóricas y Aplicadas, UNLP, CONICET, Casilla de Correo 16, Sucursal 4, (1900) La Plata, Argentina*
[3]*Institut für Physik, WA331, Johannes Gutenberg-Universität, Staudingerweg 7, D-55099 Mainz, Germany*
[4]*Institut für Theoretische Physik, Universität Göttingen, Georg-August Universität, Friedrich-Hund-Platz 1, 37077 Göttingen, Germany*
(Received 23 November 2006; published 9 May 2007)

The dynamical behavior of ferromagnetic Ising films confined in a $D\times L\times L$ geometry ($D\ll L, 1\leqslant i\leqslant D$) is studied by means of Monte Carlo simulations when either short- or long-range competing magnetic fields $H(i)$ of equal strength but opposite sign are applied at opposite walls, given by the $L\times L$ surfaces. It is well known that, for appropriate choices of the control parameters, these systems exhibit wetting phase transitions that occur in the limit of infinite film thickness at the critical curve $T_w(h_w)$, where $h_w=H(i=1)$ is the magnitude of the surface field at the wall. Results of the dynamical approach to equilibrium, at criticality and for the complete wetting regime, obtained by starting the systems from different (far-from equilibrium) initial conditions, are presented and discussed. We determine quite accurately a wetting critical point $[T_w=0.8982(57), h_w=0.555]$ for the case of short-range fields, by measuring the detachment of the wetting layer from a wall, which for this type of field obeys a logarithmic dependence on time. For retarded van der Waals forces we obtained $[T_w=0.8982, h_w=0.449(1)]$ for the critical point. The scaling behavior of the average position of the interface is also studied for the complete wetting regime at $T=0.8982$ and in the presence of a bulk magnetic field $H=1$. The numerical results are in full agreement with the theoretical expectations for the cases of short-range and long-range (both retarded and nonretarded van der Waals forces) fields, where logarithmic and power-law divergences are found, respectively.

DOI: 10.1103/PhysRevE.75.051603 PACS number(s): 05.50.+q, 61.30.Hn, 75.70.−i, 05.10.Ln

I. INTRODUCTION

When systems that undergo a phase transition in the bulk are confined in a thin film geometry, the character of the transition and the resulting ordering may be severely affected by boundary effects due to the confining walls [1–22]. For example, anisotropic ferromagnets that undergo the transition to the paramagnetic phase, fluids that undergo the vapor-liquid transition, and solid or liquid binary mixtures undergoing phase separation near their critical points all belong to the universality class [23] of the three-dimensional (3D) Ising model. In a thin film geometry, a crossover occurs [24–26] to the universality class of the two-dimensional (2D) Ising model [27]. While this crossover already results solely as an effect of spatial confinement (the linear dimension D in the direction normal to the walls being finite, true phase separation into coexisting phases via a sharp phase transition occurs only in the directions parallel to the walls), it often occurs that the walls are not "neutral" with respect to the coexisting phases, but rather "prefer" the same phase (or different ones, respectively) of the coexisting phases [17]. The case that both walls prefer the same phase (e.g., the liquid in the case of a vapor-liquid transition of a fluid) leads to a shift of the transition to conditions that would be in the one-phase region in the bulk ("capillary condensation" [1,2,4,6,10,13,17–20]). If each wall prefers a different phase, however, another type of phase transition occurs, namely, an "interface localization-delocalization transition" [3,7–9,11,12,14–17]. Already near the transition temperature T_{cb} of the bulk for finite D a gradual transition to a two-domain state occurs, where an interface forms, oriented parallel to the confining walls, separating the coexisting phases. Only at a temperature $T_c(D)$ which typically is much lower than T_{cb} does the interface get localized at one of the confining walls. For $D\to\infty$ the transition temperature $T_c(D)$ converges to the wetting transition [17,28–30] temperature T_w of the semiinfinite system. The generic example for this transition is an Ising model at zero bulk magnetic field H, but where at one of the confining surfaces a field H_1 and at the other one a field $-H_1$ acts.

While in films of finite thickness D infinitely thick wetting layers cannot form and thus the wetting transition is rounded [17], prewetting transitions [17,28–30] can survive [5,17,31], and the interplay between these transitions and the interface localization-delocalization transition may give rise to rather complicated phase diagrams of the thin film [14–17], many aspects of this behavior being still unexplored.

However, even much less is known about dynamic aspects of the ordering phenomena in this thin film geometry. Already in the bulk, it is known that anisotropic magnets, fluids, and binary fluid mixtures belong to distinct dynamic universality classes [32,33]. Here we shall only be concerned with the simplest case of relaxational behavior of a nonconserved order parameter ("model A") [32]), which can be realized by the single spin-flip kinetic Ising model [34,35]. Thus, phenomena such as surface-directed spinodal decomposition [36–42] occurring in confined binary mixtures will not be considered here; rather we are concerned with the early stages of the growth of wetting layers [43–54] (or pre-

cursors thereof). In previous work, this has been studied mostly by phenomenological theoretical considerations [43–46,48], while most previous computer simulations [50,53,54] have dealt with two-dimensional strips confined by one-dimensional boundaries. The only closely related previous work [47] dealing with the growth of wetting layers in three-dimensional Ising films considered systems with very small cross sections ($L \times L$ with $8 \leqslant L \leqslant 24$) and hence studied primarily finite size effects.

In the present work, we not only reconsider the problem posed by Mon *et al.* [47], but we also consider long-range forces due to the boundaries, in addition to the case of competing surface fields which act on the spins in the boundary planes only. In Sec. II we shall introduce the model, while Sec. III recalls the pertinent theoretical predictions. Section IV defines the quantities which are recorded, while Sec. V describes our results at zero bulk field for the case of critical wetting. Section VI contains results on the growth of precursors of wetting layers for small but nonzero bulk fields. Finally, Sec. VII summarizes our conclusions.

II. THE ISING FILM WITH COMPETING SURFACE FIELDS

The Hamiltonian $\mathcal{H}$ of the nearest-neighbor Ising model [55] on the cubic lattice, with exchange constant $J>0$ and in the presence of a magnetic bulk field (H), is given by

$$\mathcal{H} = -J \sum_{\langle n.n. \rangle}^{D,L,L} \sigma_{i,j,k}\sigma_{m,n,l} - \sum_{i=1}^{D} H(i) \sum_{jk=1}^{L,L} \sigma_{i,j,k} - H \sum_{ijk}^{D,L,L} \sigma_{i,j,k}, \tag{1}$$

where $\sigma_{i,j,k}$ are the Ising spin variables at the sites of coordinates (i,j,k), which may assume two different values, namely $\sigma_{i,j,k} = \pm 1$. The first sum of Eq. (1) runs over all the nearest-neighbor pairs of spins such that $1 \leqslant i \leqslant D$, $1 \leqslant j \leqslant L$, and $1 \leqslant k \leqslant L$. The third sum accounts for the interaction with the bulk magnetic field. Furthermore, we apply magnetic fields due to the free boundary conditions adjacent to spins in layers $i=1$ and $i=D$ [see the second sum in Eq. (1)], respectively. We studied the case of competing fields of the same magnitude that led to the observation of wetting phenomena. Furthermore, the influence of both short-range (SR)

$$H(i) = h[-\delta_{1i} + \delta_{Di}], \quad i = 1, \ldots, D \tag{2}$$

and long-range (LR)

$$H(i) = h[-i^{-p} + (D - i + 1)^{-p}], \quad i = 1, \ldots, D \tag{3}$$

boundary fields will be studied.

For the study of LR fields, we restrict ourselves to the cases $p=3$ and $p=4$ in Eq. (3). In these cases surface forces are nonretarded ($p=3$) and retarded ($p=4$) van der Waals forces [29], so that the interface located at a distance Z apart from the wall still feels a potential energy $U(Z) \propto Z^{-2}$ or Z^{-3}, respectively. We addressed these cases because there are untested theoretical predictions on the dynamic scaling behavior of Z [43,49] (see next section).

The Ising magnet in 3D and in absence of any external magnetic field, undergoes a continuous order-disorder transition at the bulk critical temperature $k_B T_{cb}/J = 4.511\,42 \pm 0.000\,05$ [56]. In the following, temperatures are reported in units of T_{cb}. However, in the confined geometry between two competing walls used in this work one observes interesting physical behavior due to the interplay between finite-size effects and criticality. In fact, for any finite value of the film thickness D the transition that would occur in the bulk at T_{cb} becomes rounded and a sharp phase transition only takes place at the size-dependent "critical" point $T_c(D)$. For $T < T_{cb}$ the surface fields cause the formation of an interface between positively and negatively magnetized regions in the ferromagnetic Ising film. Such an interface for $T < T_c(D)$ is bound either to the surface with positive or negative field with the same probability. For $T_c(D) < T < T_{cb}$, however, the interface fluctuates delocalized in the center of the film. For $T > T_{cb}$ the film is essentially disordered, except for some order close to the walls induced by the fields. So, one encounters an interface localization-delocalization transition at $T_c(D)$ that exhibits a symmetry breaking of a 2D Ising character. As $D \to \infty$, however, the critical temperature of the film converges towards the wetting transition temperature, $T_c(D) \to T_w(h_w)$ [7–9]. Therefore, while for any finite D there is a single transition at $T_c(D)$, that presumably belongs to the two-dimensional Ising universality class [12,23], in the limit $D \to \infty$ one can observe two transitions: the wetting transition at $T_w(h_w)$ and the bulk transition at T_{cb}, the latter belonging to the 3D Ising model universality class.

III. PHENOMENOLOGICAL DYNAMIC SCALING THEORY OF GROWTH OF WETTING LAYERS

Let us consider the thickness of the wetting layer $Z(t)$ as the distance from the nearest wall to the average position of the interface between magnetic domains of different orientation at time t. Then, $Z(t)$ can be expressed in terms of a dynamical scaling Ansatz [43,49] similar to the scaling approach used in domain growth [57], yielding

$$Z(t, \xi_{\parallel}) = b^{-\beta_s} Z^*(b^{-\nu_{\parallel} z} t, b \xi_{\parallel}^{-1/\nu_{\parallel}}), \tag{4}$$

where b is a scale factor, $\xi_{\parallel}$ is the correlation length for interfacial fluctuations in the direction parallel to the wall, $\nu_{\parallel}$ is the corresponding correlation length exponent, z is a dynamic exponent, and β_s is the static exponent describing the divergence of the interface distance from the wall at the wetting transition. Z^* denotes a scaling function (as well as Z^{**} and Z^{***} below). Furthermore, since in our simulations the order parameter is a nonconserved quantity one has $z=2$ [43,49].

Let us now consider two different physical situations: (i) Critical wetting, i.e., in the absence of bulk field $H=0$ and very close to the wetting critical point, and (ii) complete wetting, i.e., within the wet phase with $h > h_w$ and for $H \neq 0$.

(i) For the case of critical wetting we define $\tau = T - T_w$, so that $\xi_{\parallel}^{cw} \simeq \tau^{-\nu_{\parallel}^{cw}}$. Then, Eq. (4) becomes

$$Z(t,\tau) = b^{-\beta_s^{cw}} Z^{**}(b^{-z\nu_\parallel^{cw}} t, b\tau), \quad H \equiv 0. \tag{5}$$

Now, by taking $b = t^{1/z\nu_\parallel^{cw}}$ and considering the wetting critical point with $\tau \equiv 0$ where the second scaling variable vanishes, Eq. (5) becomes

$$Z_o(t) \simeq t^{-\beta_s^{cw}/z\nu_\parallel^{cw}}, \quad H \equiv 0. \tag{6}$$

For the case of short-range surface fields [Eq. (2)], one has $\beta_s^{cw} = 0$ and $\nu_\parallel^{cw} = 1/2$. Thus, Eq. (6) gives a logarithmic variation of the type

$$Z(t) \simeq \ln(t), \quad H \equiv 0, \quad \text{SR fields}. \tag{7}$$

On the other hand, for long-range surface fields [Eq. (3)] the exponents for nonretarded ($p=3$) and retarded ($p=4$) van der Waals forces are expected to be [43,49] $\beta_s^{cw} = -1/3$ or $-1/4$ and $\nu_\parallel^{cw} = 2/3$ or $5/8$, respectively. So, for these cases the theoretical predictions are $Z_o(t) \sim t^{1/4}$ or $Z_o(t) \sim t^{1/5}$, respectively.

(ii) For the case of complete wetting one uses $\xi_\parallel^{co} \simeq H^{-\nu_\parallel^{co}}$ and Eq. (4) yields

$$Z(t,H) = b^{-\beta_s^{co}} Z^{**}(b^{-z\nu_\parallel^{co}} t, bH). \tag{8}$$

Now, by taking $b = H^{-1}$, Eq. (8) yields

$$Z(t,H) = H^{\beta_s^{co}} Z^{***}(H^{z\nu_\parallel^{co}} t). \tag{9}$$

Again, the distinct cases of SR fields and both types of LR fields are expected to exhibit different scaling behavior depending on the corresponding critical exponents.

IV. SIMULATION DETAILS AND RECORDED QUANTITIES

The time evolution of 3D confined Ising films is simulated using the standard Metropolis algorithm. The time is measured in Monte Carlo steps (MCS), such that during one MCS all $D \times L \times L$ spins of the sample are attempted to be flipped once, on average. Simulations are started by using two kinds of initial configurations: (i) Disordered configurations corresponding to strictly zero initial magnetization, which subsequently are quenched close to the wetting critical point. (ii) Ordered configurations, with all spins pointing up, corresponding to $T=0$, which subsequently are annealed close to the wetting critical point or to a complete wetting state.

In order to study the dynamics of the delocalization of the interface we have recorded the magnetization profiles $[M(i,t), i=1,2,\cdots,D]$ measured along the D direction and averaged over the $L \times L$ planes running in the direction parallel to the walls,

$$M(i,t) = \langle \tilde{M}(i,t) \rangle = \left\langle \frac{1}{L^2} \sum_{j,k=1}^{L,L} \sigma_{ijk}(t) \right\rangle, \tag{10}$$

where $\langle\ \rangle$ corresponds to averages taken over different realizations that will be reported for each particular measurement. Also, the row magnetization describes the magnetization profiles $M(i,t), 1 \leqslant i \leqslant D$, for any desired time t. In addition to the magnetization profiles we have also measured their fluctuations, that yield the susceptibility profiles given by

$$\chi(j,t) = \langle \tilde{M}^2(j,t) \rangle - \langle \tilde{M}(j,t) \rangle^2. \tag{11}$$

Since the wetting phase diagram of the 3D Ising model with competing surface fields is not known exactly, we have performed simulations close to a previously reported critical point determined by means of Monte Carlo simulations. For this purpose we have started with SR fields and explored the neighborhood of the point $T_w \simeq 0.887$, $h_s \simeq 0.55$ [58]. We have selected this point in order to avoid possible corrections due to the bulk (pure 3D Ising) critical behavior which may become relevant close to T_{cb}. In fact, at the selected temperature the bulk correlation length is expected to be of the order of only one lattice spacing [12]. Moreover, this temperature is high enough to achieve a reasonable spin-flip rate using our standard algorithm. Furthermore, the studied temperature range is far away from the roughening temperature $T_R \simeq 0.542$ [59], so we are safely within the regime of wetting transitions, avoiding any problems due to crossover to layering transitions [60].

V. CRITICAL WETTING

A. Dynamic simulations started from ordered configurations

Figure 1(a) shows a log-log plot of $M(t)$ versus t obtained by using lattices of size $63 \times 128 \times 128$ utilizing SR surface fields. Simulations are started from a fully ordered configuration with $M_o = 1$ that corresponds to $T=0$ and the magnetization is measured when the systems are annealed at different temperatures, as indicated in the figure.

By considering that the wetting layer is at a distance $Z(t) \ll D/2$ from the wall and by assuming the formation of magnetic domains of different orientation [downward for $i < Z(t)$ and upward for $i > Z(t)$, respectively], we obtain a simple geometrical relationship between $M(t)$ and $Z(t)$, namely

$$M(t) \simeq M(0)[1 - 2Z(t)/D], \quad M(t=0) = 1. \tag{12}$$

So, according to Eq. (12), Fig. 1(b) shows plots of $[1 - M(t)]D/2$ versus t as obtained by using the data already shown in Fig. 1(a). The expected logarithmic behavior [see Eq. (7)] is found for $T=0.8982$ for three decades of time, while small—but noticeable—upward (downward) deviations are observed for $t > 10^3$ and for $T=0.9039$ ($T=0.8925$) that can be identified to correspond to the wet (nonwet) phase. So, based on the dynamical evolution of the wetting layer, our estimation for the critical point is $h_w = 0.555$ and $T_w = 0.8982(57)$. This result is in good agreement with a previous paper by Binder, Landau, and Wansleben, namely $T_w \simeq 0.887$ and $h_w \simeq 0.55$ [58].

The same procedure can be used in order to determine the wetting critical point in the case of long-range fields. However, in these cases at criticality the data should obey a power-law behavior according to Eq. (6), as shown in Fig. 2 for the case of $p=4$ in Eq. (3). The best power law is ob-

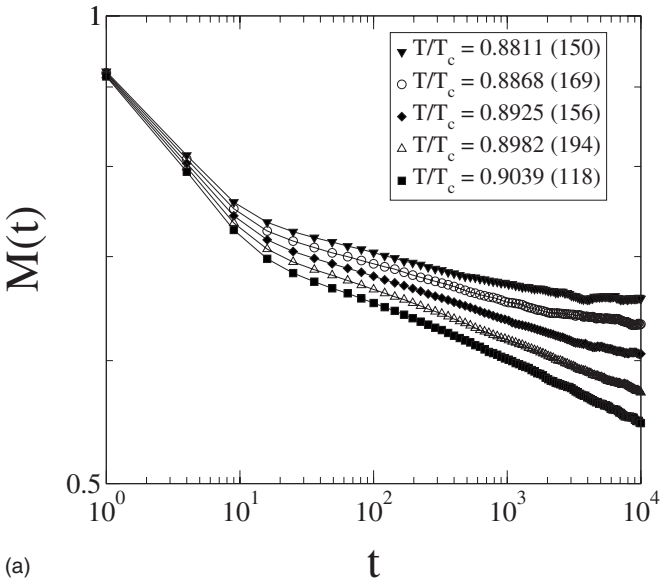

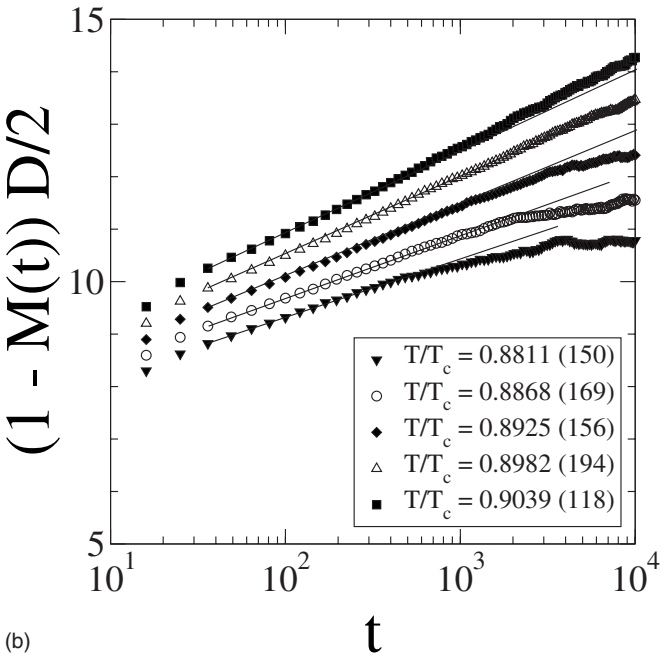

FIG. 1. (a) Log-log plot of the magnetization $M(t)$ versus t (measured in MCS). Results were obtained starting from a fully ordered configuration with $M(t=0)=1$, taking $h=0.555$ and different values of the temperature as indicated. (b) Linear-logarithmic plot of $[1-M(t)]D/2$ versus t as obtained by using the results shown in (a). The full lines show the expected logarithmic behavior according to Eq. (7) and have been drawn to guide the eyes. Results correspond to lattices of size $D=63$, $L\times L=128\times 128$, and were obtained by averaging over the number of different initial configurations, indicated by parentheses given for five temperatures.

tained for $h_w=0.449\pm0.001$ which we identify as the critical wetting point. Since here we have used the same temperature as for the case of SR fields [Fig. 1(b)], our result for the magnitude of the fields, namely $h_w^{\mathrm{SR}}>h_w^{\mathrm{LR}}$, is consistent with the long-range nature of the former fields similar to what is observed in simulations performed in two dimensions [61].

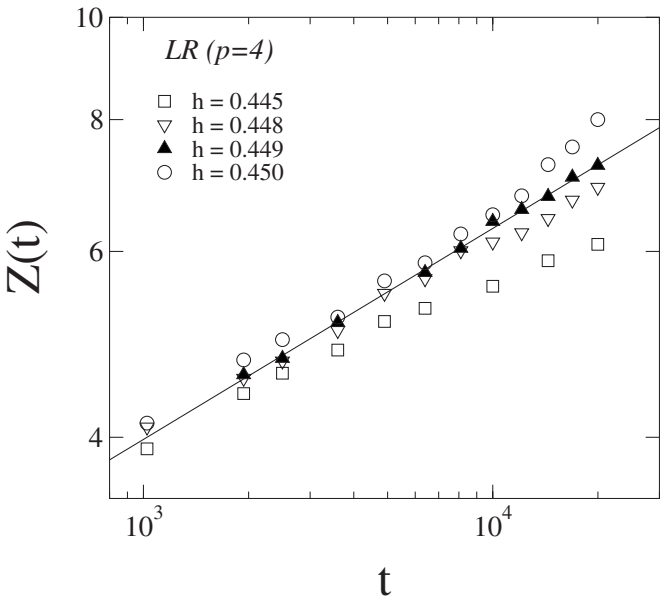

FIG. 2. Log-log plot of the position of the interface $Z(t)$ versus t (measured in MCS). Results were obtained starting from a fully ordered configuration with $M(t=0)=1$, taking $T=0.8982$ and different values of the surface magnetic field as indicated. The full line shows the expected power-law behavior according to Eq. (6) with $\beta_s=1/4$, $\nu_{\|}=5/8$, and $z=2$, and has been drawn to guide the eyes. Results correspond to lattices of size $D=76$, $L\times L=150\times 150$, and were obtained by averaging over 25 different initial configurations.

B. Dynamic simulations started from disordered configurations

In order to study the early stages of the delocalization of the interface we have measured the time evolution of the magnetization profiles, starting from fully disordered initial configurations with a total magnetization $M(t=0)=0$. The magnetization profiles, $M(i,t)$, are measured along the direction perpendicular to the walls where the fields are applied and averaged over the $L\times L$ planes parallel to the walls [see Eq. (10)]. Figure 3(a) shows plots of the row magnetization $M(i,t)$ versus time, obtained at the previously determined wetting critical point. It is observed that within a short-time regime $M(i,t)$ increases monotonically. Subsequently it reaches saturation values at least for the rows placed close to the walls, during the time scale of our measurements.

The obtained results reflect the propagation of the influence of the surface field into the bulk of the film. We expect that the average penetration distance of the perturbation into the bulk phase, $Z(t)$, that could be taken as a measure of the average position of the interface or, equivalently to the width of the growing wetting layer, should diverge logarithmically [see Eq. (7)]. In order to perform a rough test of Eq. (7) we have estimated the time required for the perturbation, $t_p(i)$, to reach the ith row, utilizing $Z(t)\equiv i$ when the row magnetization assumes the value $M(i,t_p(i))\equiv 0.2$. The values obtained using this procedure are shown in the inset of Fig. 3(a) as a linear-logarithmic plot of $Z(t)$ versus t. The full line in the inset of Fig 3(a) shows the best fit of the data given by $Z(t)=-12.67+5.34\ln(t)$. Furthermore, an additional test for

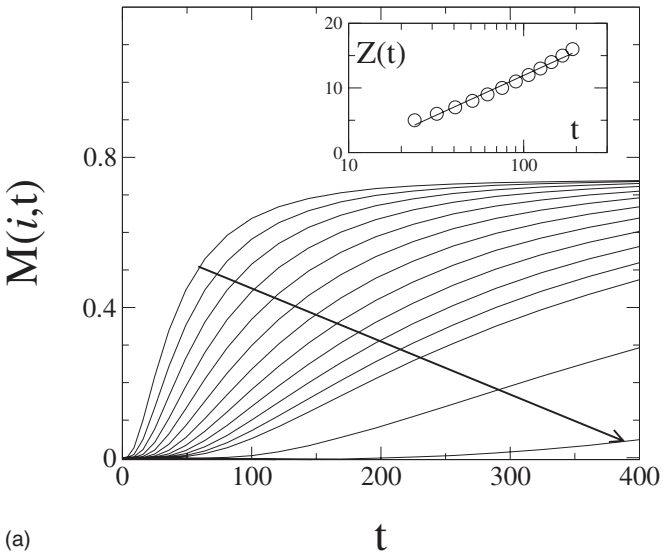

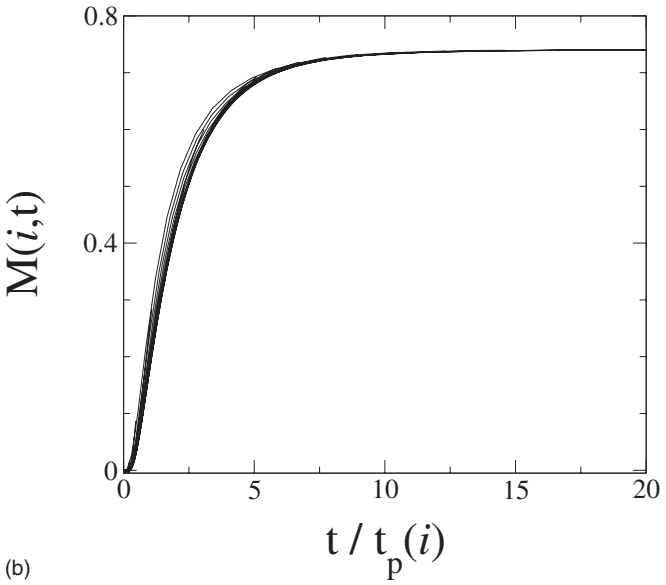

FIG. 3. (a) Plot of the row magnetization $M(i,t)$ versus time (measured in MCS). Each curve corresponds to different rows, increasing from left to right according to $i=5$, 6, 7, 8, 9, 10, 11, 12, 13, 14, 15, 16, 20, and 30, as shown by the arrow. Results were obtained for $h_w=0.555$ and $T_w=0.8982$, by using lattices of size $128\times256\times256$ and by averaging over 108 different initial disordered configurations. The inset shows a linear-logarithmic plot of $Z(t)$ versus t, as expected from Eq. (7). (b) Scaled plot of $M(i,t)$ versus $t/t_p(i)$ obtained by using the results shown in part (a). More details in the text.

the validity of the arguments discussed above can be performed by scaling the horizontal axis of Fig. 3(a) by $t_p(i)$, as shown in Fig. 3(b). The data collapse obtained is quite satisfactory, providing evidence that, in fact, the propagation of the wetting layer into the bulk diverges logarithmically.

VI. COMPLETE WETTING

In this section we present and discuss studies of the propagation of the wetting layer into the bulk within the complete wetting regime. In all cases we have taken $T=0.8982$, $h=1.00$ and varied the magnetic field in the bulk. The thickness of the wetting layer measured by the interface position $Z(t)$, as well as the *effective* width of the interface, $w(t)$, are obtained from the magnetization profile just by fitting the numerical curves to an error function [61,62],

$$M(i,t) = -M_0 \,\mathrm{erf}\left(\frac{\sqrt{\pi}[i-Z(t)]}{2w(t)}\right), \tag{13}$$

where the constant M_0 is of the order of the bulk magnetization and is obtained for $i>D/2$.

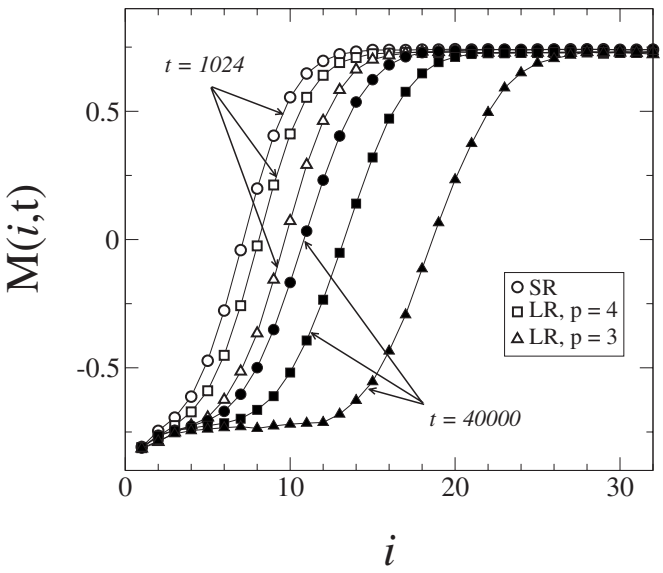

FIG. 4. Plot of the magnetization profiles $M(i,t)$ versus the distance from the wall (i, measured in lattice spaces). Data corresponding to SR and LR surface magnetic fields are shown for $t=1024$ MCS and $t=40\,000$ MCS, as indicated. Results were obtained for $h=1.0$, $T_w=0.8982$, and $H=0.0001$, by using lattices of size $64\times128\times128$ and by averaging over 20 different initial configurations. More details in the text.

In order to gain insight into the behavior of the magnetization profiles for different physical situations, it is worthwhile to analyze some typical examples, as shown in Fig. 4 for the three types of surface magnetic fields used in this work. Also, for the sake of comparison we have included measurements performed at two different times, namely $t=1024$ MCS and $t=40\,000$ MCS, while in all cases one has $H=0.0001$.

In Fig. 4 one observes qualitatively the different rates of propagation of the wetting layers into the bulk. The profiles corresponding to SR fields remain closer to the wall since in this case the interface position diverges only logarithmically [Eq. (7)]. On the other hand, the fastest divergence of the interface position, $Z(t)\propto t^{1/4}$, is expected to occur for LR fields with $p=3$ in Eq. (3), in agreement with the largest displacements of the corresponding profiles. Moreover, for $p=4$ in Eq. (3) one has a weaker power-law divergence, $Z(t)\propto t^{1/5}$, and the profiles lie always between the two preceding cases.

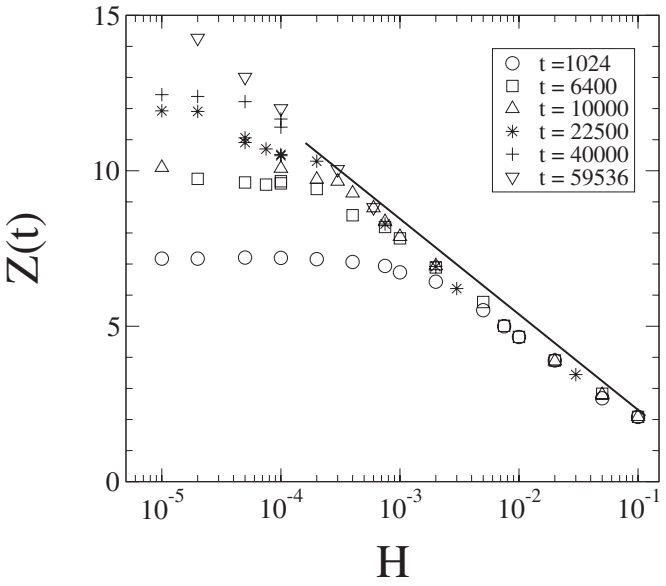

FIG. 5. Linear-logarithmic plot of the average position of the wetting layer $Z(t)$ versus the bulk magnetic field H. Data corresponding to SR surface magnetic fields are shown for different times as indicated. Results were obtained for $h=1.0$ and $T=0.8982$ by using lattices of size $64\times128\times128$ and by averaging over 20 different initial configurations. The full line shows the expected behavior according to Eq. (9) and has been drawn to guide the eyes. More details in the text.

Now, by fitting magnetization profiles, as those shown in Fig. 4, with the aid of Eq. (13) we can analyze the detachment of the wetting layer from the wall. In fact, Figs. 5–7 show plots of $Z(t)$ versus the bulk field (H) as obtained for the three different magnetic surface fields studied in this work, namely SR, LR ($p=4$), and LR ($p=3$), respectively.

For the case of SR fields (Fig. 5) one finds that for large enough bulk fields the data follow the logarithmic dependence, as expected from Eq. (9) with $\beta_s^{co}=0$, independently of the measurement time according to the fact that the scaling function should behave as $Z^{***}(H^{z\nu_\parallel^{co}}t)=Z^{***}(u)=$constant for $u\gg1$. Also, in the limit of weak fields, the data show saturation effects evidenced by different levels of plateaus, that on the one hand are independent of the bulk field, but, on the other hand, depend on the measurement time. This observation corresponds to the behavior expected for the free interface regime and the plateaus indicate the maximal distances reached by the free interfaces at a given time. Also, Figs. 6(a) and 7(a) show plots of the average position of the interface $Z(t)$ versus the bulk magnetic field H as obtained for different times for the cases of LR fields with $p=4$ and $p=3$, respectively. For these cases one observes the same qualitative behavior as for SR fields [Fig. 6(a)], however the asymptotic regime for large fields obeys a power law that is compatible with $\beta_s^{co}=0=-1/4$ and $\beta_s^{co}=-1/3$ in Eq. (9) for $p=4$ and $p=3$, respectively.

In addition the data obtained within the complete wetting regime allow us to test the validity of the scaling relation given by Eq. (9), as shown in Figs. 6(b) and 7(b). In both cases we obtained an acceptable data collapse strongly supporting the validity of the scaling Ansatz.

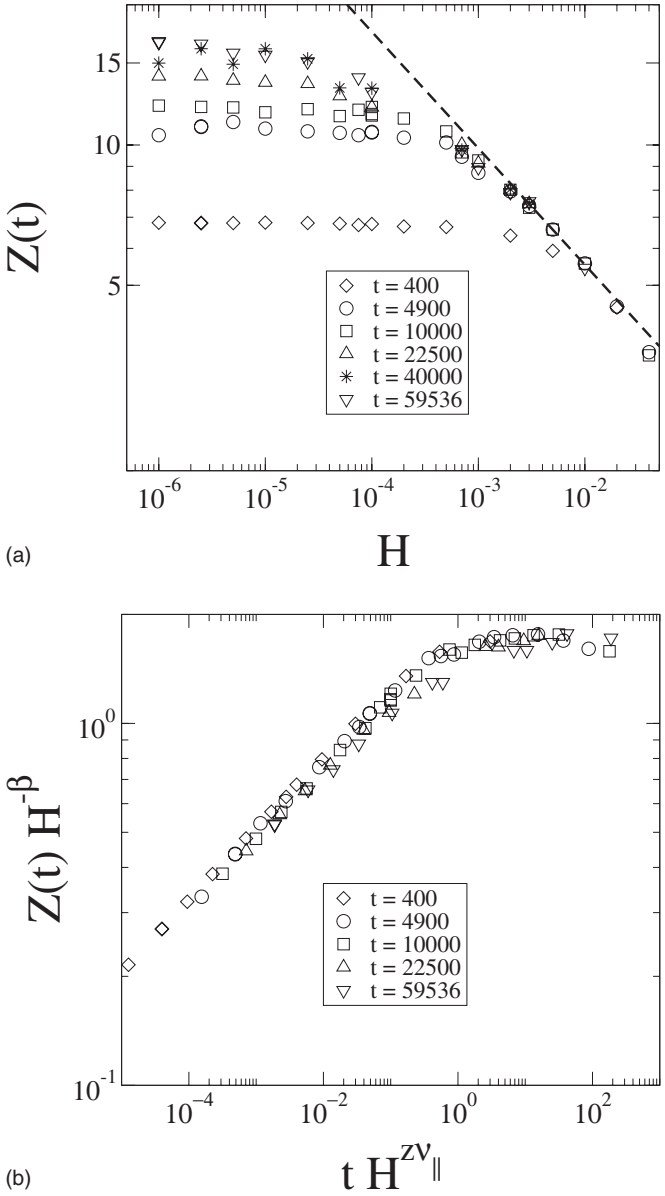

FIG. 6. (a) Log-log plot of the average wetting layer thickness $Z(t)$ versus the bulk magnetic field H. Data corresponding to LR surface magnetic fields with $p=4$ in Eq. (3) are shown for different times as indicated. Results were obtained for $h=1.0$ and $T=0.8982$ by using lattices of size $64\times128\times128$ and by averaging over 20 different initial configurations. The dashed line shows the expected behavior according to Eq. (9) and has been drawn to guide the eyes. More details in the text. (b) Data collapse of the results shown in (a) obtained by using the scaling law given by Eq. (9).

VII. CONCLUSIONS

In this paper thin ferromagnetic Ising films with nearest-neighbor interactions and free surfaces at which competing surface fields act, Eqs. (2) and (3), have been considered. Extensive Monte Carlo simulations were presented and analyzed which elucidate the dynamics of the growth of wetting layers, starting the simulation of these model systems in an initial condition with all spins pointing up corresponding to a nonwet state of the surface or, alternatively, in a disordered

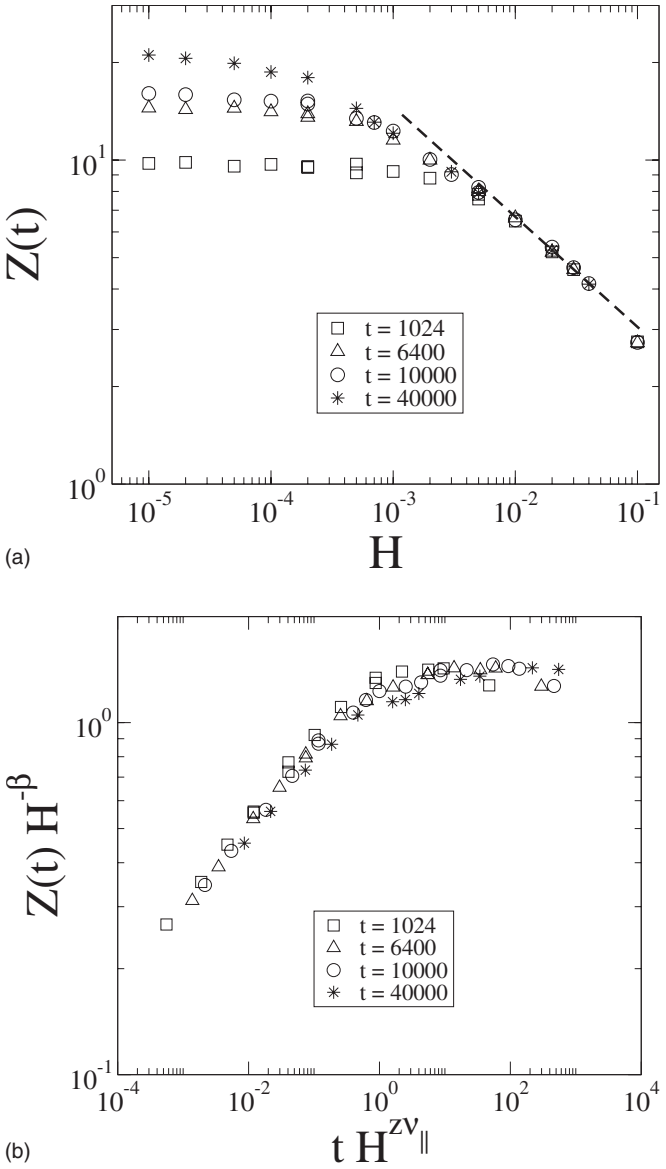

FIG. 7. (a) Log-log plot of the average position of the wetting layer $Z(t)$ versus the bulk magnetic field H. Data corresponding to LR surface magnetic fields with $p=3$ in Eq. (3) are shown for different times as indicated. Results were obtained for $h=1.0$ and $T=0.8982$ by using lattices of size $64\times128\times128$ and by averaging over 20 different initial configurations. The dashed line shows the expected behavior according to Eq. (9) and has been drawn to guide the eyes. (b) Data collapse of the results shown in (a) obtained by using the scaling law given by Eq. (9). More details in the text.

spin configuration, corresponding to a quenching experiment from the paramagnetic phase to a state exactly at the phase boundary for the critical wetting transition of the model system.

The case where the surface field acts on the surface planes only, Eq. (2), is the generic model for critical wetting with short-range forces, a problem which has been extensively studied in the literature. In this case the scaling theory due to Lipowsky [43] predicts a logarithmic growth law for the thickness of the wetting layer with time. Our results confirm this prediction nicely (Fig. 1) and also demonstrate a scaling behavior of the order parameter profile, when we start from disordered configurations (Fig. 3). For a surface field which decays with a power law of the distance from the surface (as expected for van der Waals forces), we confirm the predicted power law for the growth of the wetting layer (Fig. 2).

Also the growth of wetting layers under conditions deep within the complete wetting regime has been studied. It is found that the order parameter profile can be approximated by an error function, Eq. (13), where both the mean interface position $Z(t)$ and its width $w(t)$ increase with time. Also these studies were performed both for short-range surface fields, Eq. (2), and for power laws, Eq. (3), corresponding to either retarded or nonretarded van der Waals forces. Again the simulation results are well compatible with the corresponding theoretical predictions, when we study the scaling behavior as a function of the applied bulk field (Figs. 5 and 6).

Thus, we conclude that the theory of Lipowsky [43] on the growth of wetting layers in the case of a simple nonconserved order parameter with relaxational dynamics is fully consistent with our Monte Carlo data. Nevertheless, the present work is only a first step towards the description of wetting layer growth in a real system. For example, for solid binary mixtures conservation of the concentration of the species needs to be taken into account, and for wetting phenomena in fluids hydrodynamic transport plays an important role. Modelling of the latter case requires the use of molecular dynamics methods (e.g., Ref. [42]), but this is possible so far only for much smaller systems than are accessible for the present lattice model with Monte Carlo methods. In view of the simplified character of our model and its dynamics, it would be premature to attempt a direct comparison of our results with experimental data (e.g., Ref. [52]) at this point. Nevertheless, we feel it is reassuring that our simulations confirm the phenomenological theories and scaling concepts, and presumably the latter can be suitably carried over to more complex real systems as well.

ACKNOWLEDGMENTS

This work is supported financially by CONICET, UNLP, and ANPCyT (Argentina). One of the authors (E.V.A.) acknowledges the DAAD (Germany) for financial support under the DAAD-CONICET scientific exchange program and the Alexander von Humboldt Foundation (Germany).

[1] M. E. Fisher and H. Nakanishi, J. Chem. Phys. **75**, 5857 (1981).
[2] R. Evans and P. Tarazona, Phys. Rev. Lett. **52**, 557 (1984).
[3] E. V. Albano, K. Binder, D. W. Heermann, and W. Paul, Surf. Sci. **223**, 151 (1989).
[4] E. V. Albano, K. Binder, D. W. Heermann, and W. Paul, J. Chem. Phys. **91**, 3700 (1989).
[5] D. Nicolaides and R. Evans, Phys. Rev. B **39**, 9336 (1989).
[6] R. Evans, J. Phys.: Condens. Matter **2**, 8989 (1990).
[7] A. O. Parry and R. Evans, Phys. Rev. Lett. **64**, 439 (1990).
[8] M. R. Swift, A. L. Owczarek, and J. O. Indekeu, Europhys. Lett. **14**, 475 (1991).
[9] A. O. Parry and R. Evans, Physica A **181**, 250 (1992).
[10] K. Binder and D. P. Landau, J. Chem. Phys. **96**, 1444 (1992).
[11] K. Binder, D. P. Landau, and A. M. Ferrenberg, Phys. Rev. Lett. **74**, 298 (1985); Phys. Rev. E **51**, 2823 (1995).
[12] K. Binder, R. Evans, D. P. Landau, and A. M. Ferrenberg, Phys. Rev. E **53**, 5023 (1996).
[13] L. D. Gelb, K. E. Gubbins, R. Radhakrishnan, and M. Sliwinska-Barthkowiak, Rep. Prog. Phys. **62**, 1573 (1999).
[14] M. Müller, K. Binder, and E. V. Albano, Physica A **279**, 188 (2000); M. Müller, E. V. Albano, and K. Binder, Phys. Rev. E **62**, 5281 (2000).
[15] M. Müller, K. Binder, and E. V. Albano, Europhys. Lett. **49**, 724 (2000).
[16] M. Müller and K. Binder, Phys. Rev. E **63**, 021602 (2001).
[17] K. Binder, D. P. Landau, and M. Müller, J. Stat. Phys. **110**, 1411 (2003).
[18] M. Schmidt, A. Fortini, and M. Dijkstra, J. Phys.: Condens. Matter **15**, S3411 (2003); **16**, S4159 (2004).
[19] R. L. C. Vink, K. Binder, and J. Horbach, Phys. Rev. E **73**, 056118 (2006).
[20] R. L. C. Vink, A. De Virgiliis, J. Horbach, and K. Binder, Phys. Rev. E **74**, 031601 (2006).
[21] For recent reviews, see Refs. [13,17,22].
[22] D. P. Landau, in *Computer Simulations of Surfaces and Interfaces*, NATO Science Series II, edited by B. Dünweg, D. P. Landau, and A. Milchev (Kluwer Academic, Dordrecht, 2003), Vol. 114, p. 261; K. Binder, *ibid.*, p. 275.
[23] M. E. Fisher, Rev. Mod. Phys. **46**, 587 (1974).
[24] K. Binder, Thin Solid Films **20**, 367 (1974).
[25] Y. Rouault, J. Baschnagel, and K. Binder, J. Stat. Phys. **80**, 1009 (1995).
[26] F. Freire, D. O'Connor, and C. R. Stephens, J. Stat. Phys. **74**, 219 (1994).
[27] B. M. McCoy and T. T. Wu, *The Two-Dimensional Ising Model* (Harvard University Press, Cambridge, MA, 1973).
[28] P. G. de Gennes, Rev. Mod. Phys. **57**, 827 (1985).
[29] S. Dietrich, in *Phase Transitions and Critical Phenomena*, edited by C. Domb and J. L. Lebowitz (Academic, London, 1988), Vol. 12.
[30] See Telo da Gama, in *Computer Simulations of Surfaces and Interfaces*, Ref. [22], p. 239.
[31] K. Binder, Annu. Rev. Phys. Chem. **43**, 33 (1992).
[32] P. C. Hohenberg and B. I. Halperin, Rev. Mod. Phys. **49**, 435 (1977).
[33] A. Onuki, *Phase Transition Dynamics* (Cambridge University Press, Cambridge, 2002).
[34] R. J. Glauber, J. Math. Phys. **4**, 294 (1963).
[35] K. Kawasaki, in *Phase Transitions and Critical Phenomena*, edited by C. Domb and M. S. Green (Academic, London, 1972), Vol. 2.
[36] R. A. L. Jones, L. J. Norton, E. J. Kramer, F. S. Bates, and P. Wiltzius, Phys. Rev. Lett. **66**, 1326 (1991).
[37] S. Puri and K. Binder, Phys. Rev. A **46**, R4487 (1992).
[38] For reviews, see S. Puri, J. Phys.: Condens. Matter **17**, R101 (2005); also see Refs. [39–41].
[39] G. Krausch, Mater. Sci. Eng., R. **14**, 1 (1995).
[40] K. Binder, J. Non-Equilib. Thermodyn. **23**, 1 (1998).
[41] M. Geoghegan and G. Krausch, Prog. Polym. Sci. **28**, 261 (2003).
[42] S. K. Das, S. Puri, J. Horbach, and K. Binder, Phys. Rev. Lett. **96**, 016107 (2006); Phys. Rev. E **73**, 031604 (2006); **72**, 061603 (2005).
[43] R. Lipowsky, J. Phys. A **18**, L585 (1985).
[44] R. Lipowsky and D. A. Huse, Phys. Rev. Lett. **57**, 353 (1986).
[45] I. Schmidt and K. Binder, Z. Phys. B: Condens. Matter **67**, 369 (1987).
[46] M. Grant, K. Kaski, and K. Kankaala, J. Phys. A **20**, L571 (1987).
[47] K. K. Mon, K. Binder, and D. P. Landau, Phys. Rev. B **35**, 3683 (1987).
[48] M. Grant, Phys. Rev. B **37**, 5705 (1988).
[49] K. Binder, in *Kinetics of Ordering and Growth at Surfaces*, edited by M. G. Lagally (Plenum, New York, 1990), p. 31.
[50] E. V. Albano, K. Binder, D. W. Heermann, and W. Paul, J. Stat. Phys. **61**, 161 (1990).
[51] A. Patrykiejew and K. Binder, Surf. Sci. **273**, 413 (1992).
[52] H. K. Pak and B. M. Law, Europhys. Lett. **31**, 19 (1995).
[53] E. V. Albano, A. De Virgiliis, M. Müller, and K. Binder, J. Phys.: Condens. Matter **16**, 3853 (2004).
[54] E. V. Albano, A. De Virgiliis, M. Müller, and K. Binder, J. Phys.: Condens. Matter **18**, 2761 (2005).
[55] E. Ising, Z. Phys. **31**, 253 (1925).
[56] A. M. Ferrenberg and D. P. Landau, Phys. Rev. B **44**, 5081 (1991).
[57] A. Sadiq and K. Binder, J. Stat. Phys. **35**, 517 (1984).
[58] K. Binder, D. P. Landau, and S. Wansleben, Phys. Rev. B **40**, 6971 (1989).
[59] E. Bürkner and D. Stauffer, Z. Phys. B: Condens. Matter **55**, 241 (1983); K. K. Mon, S. Wansleben, D. P. Landau, and K. Binder, Phys. Rev. B **39**, 7089 (1989); K. K. Mon, D. P. Landau and D. Stauffer, *ibid.* **42**, 545 (1990).
[60] K. Binder and D. P. Landau Phys. Rev. B **46**, 4844 (1992).
[61] A. De Virgiliis, E. V. Albano, M. Müller, and K. Binder, J. Phys.: Condens. Matter **17**, 4579 (2005).
[62] E. V. Albano, A. De Virgiliis, M. Müller, and K. Binder, Physica A **352**, 477 (2004).